

RETAKE: Reducing Temporal and Knowledge Redundancy for Long Video Understanding

Xiao Wang^{1*†} Qingyi Si^{2*} Jianlong Wu¹ Shiyu Zhu³ Li Cao² Liqiang Nie^{1‡}

¹Harbin Institute of Technology, Shenzhen

²Huawei Technologies Co., Ltd. ³Shandong University

scz.wangxiao@gmail.com, siqingyi@huawei.com, wujianlong@hit.edu.cn

xyzcaoli@outlook.com, nieliqiang@gmail.com

Abstract

Video Large Language Models (VideoLLMs) have achieved remarkable progress in video understanding. However, existing VideoLLMs often inherit the limitations of their backbone LLMs in handling long sequences, leading to challenges for long video understanding. Common solutions either simply uniformly sample videos' frames or compress visual tokens, which focus primarily on low-level temporal visual redundancy, overlooking high-level knowledge redundancy. This limits the achievable compression rate with minimal loss. To this end, we introduce a training-free method, **RETAKE**, containing two novel modules **DPSelect** and **PivotKV**, to jointly model and reduce both temporal visual redundancy and knowledge redundancy for long video understanding. Specifically, **DPSelect** identifies keyframes with local maximum peak distance based on their visual features, which are closely aligned with human video perception. **PivotKV** employs the obtained keyframes as pivots and conducts KV-Cache compression for the non-pivot tokens with low attention scores, which are derived from the learned prior knowledge of LLMs. Experiments on benchmarks VideoMME, MLVU, and LVBench, show that **RETAKE** can support 4x longer video sequences with minimal performance loss (< 1%) and outperform all similar-size VideoLLMs with 3%-5%, even surpassing or on par with much larger ones. Our code is available at <https://github.com/SCZwangxiao/video-ReTake>.

1. Introduction

In the pursuit of general intelligence, Video Large Language Models [18, 22, 28, 48] have revolutionized video understanding. These models are typically extensions of Mul-

timodal Large Language Models (MLLMs), which integrate visual encoders with Large Language Models (LLMs) through instruction tuning [23] to manage multimodal tasks. However, the nature of current MLLMs requires hundreds of tokens to represent a single image [16, 39], making it impractical to process videos longer than several minutes. Specifically, the context length of common MLLMs [16, 39] limits their ability to handle only short videos of around 4 minutes at 240 frames.

To empower VideoLLMs to process longer videos, Lin et al. [22] and Li et al. [19] simply adopt sparse sampling, selecting a fixed number of frames uniformly across the video length. This approach overlooks the spatial details within frames and the temporal structure of different short-term segments, leading to a coarse and incomplete understanding of long videos [43]. To enable dense frame sampling, some methods [35, 49] have tried to extend the context length of MLLMs through long context post-training. However, training on long video data imposes extremely high requirements on infrastructure capabilities or requires complex design of distributed training systems and algorithms [45]. Therefore, recent methods [11, 14, 36, 43] compress visual tokens to fit more frames into VideoLLM within existing GPU memory limits, including token sparsification both between and within frames [14] or using visual token compressors like Q-Former [18]. However, these methods mainly focus on spatial and temporal visual redundancies [41, 53], which are low-level and limit compression rates without significant information loss.

A potential solution to above limitations is **Reducing Temporal and Knowledge redundancy**. Unlike previous methods, **RETAKE** is oriented to solving both low-level temporal redundancy and high-level knowledge redundancy. Inspired by the fact that language has higher information density than vision and is a higher-level knowledge representation, we believe that the vision-language alignment process of MLLMs forces them to learn high-level

*Equal contribution.

†Work done during an internship at Huawei.

‡Corresponding author.

judgment on knowledge redundancy, which involves abstract patterns or structures that can be inferred from human prior knowledge [10], allowing for better compression ratios with smaller minimal loss. To achieve this previously overlooked solution, we introduce a novel RETAKE framework for enhanced long video understanding, comprising two training-free components: **DPSelect** and **PivotKV**.

Specifically, to reduce low-level temporal redundancy, DPSelect is proposed to extract keyframes based on their vision encoder features. In contrast to previous methods [11] that select keyframes by identifying frames with the top-N maximum cosine distance between adjacent frames, DPSelect identifies frames with local maximum (peaks) distance, hence the name “Dist Peak Select”. This strategy is more closely aligned with human video perception, which tracks the peak stimulus to detect motion [27]. On the basis of DPSelect, to reduce high-level knowledge redundancy, we develop PivotKV, a KV cache compression technique for VideoLLM to reduce the multimodal context length. Unlike existing KV cache compression techniques for LLM [20, 51], PivotKV employs keyframes from DPSelect as pivots during compression to prevent loss of low-level visual details. Specifically, we divide the video into several segments, and apply chunked prefilling for each segment. In this process, PivotKV compresses tokens within each chunk, where keyframe tokens remain uncompressed as pivots, while other tokens are compressed based on their attention scores. Such attention score implicitly reflects the redundancy of each token as identified by the MLLM’s high-level multimodal knowledge. RETAKE allows the VideoLLM to process more frames within the GPU memory constraints for better long video understanding.

We conduct extensive experiments across various video understanding benchmarks, including VideoMME [9], MLVU [52], and LongVideoBench [44]. Results show that RETAKE can support 4x longer video sequence with less than 1% performance drop, and significantly outperforms videoLLMs of similar sizes by 3%-5%, such as MiniCPM-V2.6-8B [46] and LLaVA-OneVision-7B [16]. Even surpass or on par with much larger models InternVL2-34B [13] and VideoLLaMA 2-72B [7]. Ablation study validates the effectiveness of DPSelect and PivotKV: DPSelect can better preserve low-level visual details during compression which is important for the action reasoning and attribute perception tasks. For general tasks, PivotKV can achieve a 2x compression rate than DPSelect under the same performance drop. In summary, our contributions are threefold:

- To our best knowledge, the proposed training-free RETAKE is the first to jointly model temporal and knowledge redundancy for long video understanding, which enables 4x longer video sequence with less than 1% performance drop.
- We propose a novel keyframe selection method DPSelect

to reduce low-level temporal redundancy, and a novel KV Cache compression method PivotKV to reduce high-level knowledge redundancy in long videos.

- Our approach has outperformed similar-sized VideoLLMs by 3%-5% on various challenging video understanding tasks, setting new state-of-the-art benchmarks.

2. Related Work

2.1. Video Large Language Models

Most videoLLMs are built upon image MLLMs and further trained to capture the temporal relationships between video frames by learning from video-text pairs. A VideoLLM generally consists of a vision foundational model (VFM) [30], a LLM [8] and an intermediate connector that links the two. The VFM is responsible for extracting visual features from input video, while the connector maps these features into a representation that the LLM can process, enabling the LLM to leverage its generalization capabilities for video understanding. Based on the type of connector used, VideoLLMs can be classified into two main types: concatenation-based models and Q-Former-based models. Concatenation-based approaches [22, 24, 28] is straightforward and effective, but it faces the challenge of exponentially increasing computational costs as the sequence length grows, making it unsuitable for long video sequences. Q-Former-based models [18, 19] leverage a transformer decoder with learnable tokens to compress the VFM patch embeddings. Their performance is generally lower due to information loss during compression.

2.2. Long Video Understanding

VideoLLM community has explored three primary approaches to address the long video understanding. (1) *Sparse sampling*. Early videoLLMs can be directly applied to long video benchmarks [9, 44, 52] without any modification. For example Video-LLaVA [22] and VideoChat2 [19] process a video with arbitrary length by uniformly sampling 8 and 16 frames respectively. Obviously, sparse sampling inevitably discards a larger proportion of frames as video length increases, disrupting intrinsic temporal structures and leading to a fragmented understanding of long videos [49]. (2) *Length extrapolation*. To extend VideoLLMs’ ability for dense sampling, recent works [35, 45, 49] post-trains videoMLLMs with long-sequence data to extend context length, enabling them to process more visual tokens, resulting in a more proficient understanding for long videos. However, while effective, length extrapolation cannot overcome the quadratically increasing computational demands. (3) *Multimodal context compression*. To help VideoLLMs process more frames within GPU memory limits by extracting key information, Weng et al. and Li et al. [21, 43] reduce token counts by averaging adjacent temporal tokens, pre-

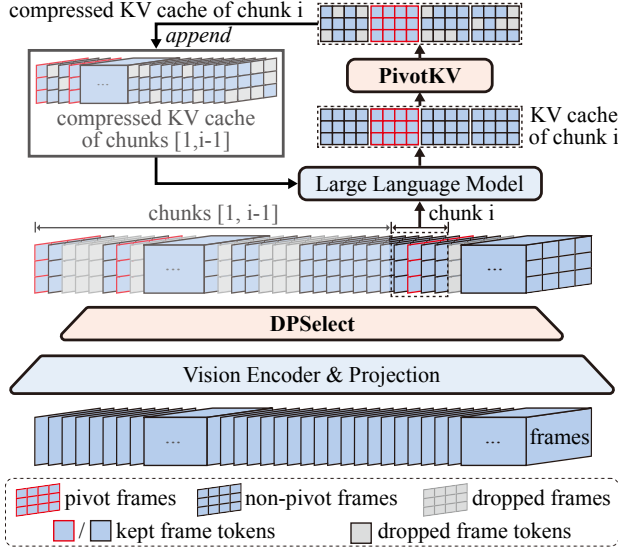


Figure 1. Illustration of ReTaKe.

serving key information. Jin et al. and Ren et al. [14, 32] further optimize video representations by merging non-essential visual tokens both within and across frames. Song et al. and He et al. [11, 36] use a memory bank to iteratively merge and store visual tokens. However, their compression rate is limited by reliance on low-level visual redundancy.

To summarize, given a computational budget, multi-modal context compression emerges as an effective strategy for achieving long video understanding. However, current methods lack the incorporation of high-level world knowledge, which hampers the accurate extraction of key information, thus constraining both the compression rate and performance. Our approach addresses it by simultaneously managing low- and high-level redundancies.

3. Method

3.1. Overview

The overall architecture of RETAKE is illustrated in Figure 1. DPSelect first extracts keyframes with local maximum distance based on their vision encoder features. PivotKV then compresses tokens within each chunk, where keyframe tokens remain uncompressed as pivots, while other tokens are compressed based on their attention scores.

Algorithm 1 outlines the general pipeline of our RETAKE framework, including five steps: video encoding, DPSelect video compression, video-text splitting & chunking, chunked prefill, and decoding. In the DPSelect video compression step, keyframes are selected using DPSelect (Section 3.3) to compress the video, reducing temporal redundancy. Similar to standard LLM pipelines described in Section 3.2, chunked prefill encodes input videos and prompts, while decoding generates answers. The key difference is

Algorithm 1 RETAKE Algorithm

- 1: **Input:** Video frames $\mathbf{F} \in \mathbb{R}^{T \times 3}$, prompt embeddings $\mathbf{P} \in \mathbb{R}^{L \times d}$, DPSelect compression ratio $\alpha_{dp} \in (0, 1]$, and PivotKV compression ratio $\alpha_{kv} \in (0, 1]$. Visual encoder with projection VE, visual-text concatenator VTC, and large language model LLM.
 - 2: **Output:** Generated output O .
 - 3: // Step 1: Video encoding
 - 4: $\mathbf{M} \in \mathbb{R}^{T \times N \times d} \leftarrow \text{VE}(\mathbf{F})$
 - 5: // Step 2: DPSelect video compression
 - 6: $\hat{\mathbf{M}} \in \mathbb{R}^{T \times \alpha_{dp} N \times d} \leftarrow \text{DPSelect}(\mathbf{M}, \alpha_{dp})$
 - 7: // Step 3: Chunking: Split text and video tokens, chunk video into segments
 - 8: $\mathbf{H} \in \mathbb{R}^{T \times (\alpha_{dp} N + L) \times d} \leftarrow \text{VTC}(\mathbf{P}, \mathbf{M})$
 - 9: $\mathcal{H} = [\mathbf{H}_1, \mathbf{H}_2, \dots, \mathbf{H}_C] \leftarrow \mathbf{H}$
 - 10: // Step 4: Chunked prefill
 - 11: Initialize an empty KVCache $\mathbf{K} \in \mathbb{R}^{0 \times d}$
 - 12: **for** \mathcal{H}_i in \mathcal{H} **do**
 - 13: $\mathbf{K} \leftarrow \text{LLM}(\mathcal{H}_i, \mathbf{K})$
 - 14: **if** \mathcal{H}_i is video chunk **then**
 - 15: $\mathbf{K} \leftarrow \text{PivotKV}(\mathbf{K}, \alpha_{kv})$
 - 16: **end if**
 - 17: **end for**
 - 18: // Step 5: Decoding
 - 19: $O \leftarrow \text{LLM}(\mathbf{K})$
 - 20: **return** O
-

our use of chunked prefill to process video and text separately, which is mathematically equivalent to standard prefill [47]. During chunked prefill, we apply PivotKV (Section 3.4) to compress the video KVCache, reducing knowledge redundancy by leveraging world knowledge in LLM.

3.2. Preliminaries

Similar to LLM, the inference process of VideoLLM consists of two phases: **prefill** and **decoding**.

Prefill phase. The prefill phase processes initial input tokens by computing self-attention for each token in an autoregressive manner. In this approach, the representation of each token in each layer depends solely on its preceding tokens. Thus, to reduce peak memory usage, we can implement **chunked prefill**, where the input tokens are divided into chunks. VideoLLM then processes each chunk autoregressively, which is mathematically equivalent to the standard prefilling [47].

Decoding phase. The decoding phase involves generating text from an initial input by predicting subsequent tokens in a step-by-step, autoregressive manner. This process utilizes a self-attention mechanism to consider the context of previously generated tokens. Due to the autoregressive nature of

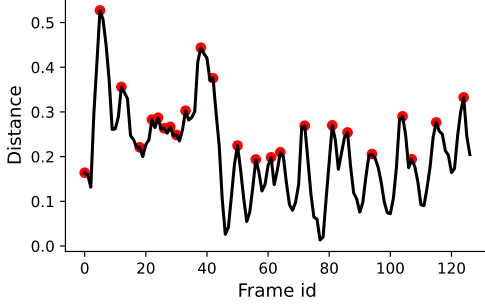


Figure 2. Illustration of DPSelect. Distance represents cosine dissimilarity between the i -th and $i + 1$ -th frames.

VideoLLM, the representation of each token in each layer depends solely on its preceding tokens. Thus we can avoid re-computing the key and value states of all previous tokens by storing them in a cache, namely **KV cache** (Key-Value cache). KV cache is calculated during both the prefill and decode phases.

3.3. DPSelect

To reduce low-level temporal redundancy, DPSelect is proposed to extract keyframes based on vision encoder features, as illustrated in Figure 2. Given a long sequence of input video features $\mathbf{M} \in \mathbb{R}^{T \times N \times C}$ containing T frames, each frame consists of N tokens with dimension size of C , DPSelect aims to compress it into a shorter sequence with minimal information loss $\mathbf{M}' \in \mathbb{R}^{t \times N \times C}$, where $t < T$. We first compute the mean pooled distance matrix between adjacent frame features as follows:

$$\bar{D}_i = \frac{1}{N} \sum_{j=1}^N (1 - \cos(\mathbf{m}_{i,j}, \mathbf{m}_{i+1,j})). \quad (1)$$

Then max pooling is used to identify local maxima positions as candidate keyframes \mathcal{P} , which is closely aligned with human video perception:

$$\mathcal{P} = \arg \max_{w_i} (\bar{D}_{w_i}), \quad w_i = [i - \lfloor W/2 \rfloor, i + \lfloor W/2 \rfloor], \quad (2)$$

where W is the window size of max pooling. Then we filter out the final keyframes \mathcal{K} such that the compressed number of time steps does not exceed t :

$$\mathcal{K} = \text{top-k}(\bar{D}[\mathcal{P}], k = t). \quad (3)$$

Finally, we extract the new video sequence \mathbf{M}' and corresponding mask \mathbf{Mask} based on the selected keyframes:

$$\mathbf{M}'_k = \mathbf{M}_{\mathcal{K},k}, \quad \forall k \in [1, N] \quad (4)$$

$$\mathbf{Mask}_k = \begin{cases} 1 & \text{if } k \in \mathcal{K} \\ 0 & \text{otherwise} \end{cases} \quad (5)$$

3.4. PivotKV

After DPSelect, we have keyframes by simulating human cognitive activities and the corresponding mask, \mathbf{M} . Next, we feed them into PivotKV to further compress the token sequence based on the keyframes and the attention mechanism, where implicitly reflects the redundancy as identified by the MLLM’s high-level multimodal knowledge.

Given the batch size b , the number of query heads h_q and key/value heads h_k/h_v , the lengths of the query sequence l_q and key sequence l_k , and head dim d . Additionally, $\mathbf{K}_{\text{cache}}$ and $\mathbf{V}_{\text{cache}}$ represent the key-value cache. First, we compute the number of key-value pairs to retain based on the pre-defined compression ratio $\alpha \in [0, 1]: l' = \lfloor \alpha \cdot l_q \rfloor$.

Next, we calculate the attention weights matrix $\mathbf{A} \in \mathbb{R}^{b \times h_q \times l_q \times l_k}$ between the query states and the most recent key states:

$$\mathbf{A} = \text{softmax} \left(\frac{\mathbf{Q} \cdot \mathbf{K}_{\text{cache},:, -l_q:, :}^\top}{\sqrt{d}} \right). \quad (6)$$

To reduce differences across heads, we sum and average the attention weights along the head dimension:

$$\bar{\mathbf{a}} = \frac{1}{h_k} \sum_{i=1}^{h_k} \mathbf{A}_{0,i, :, :} \quad (7)$$

After that, the mask $\mathbf{M} \in \{0, 1\}^{h_k \times l_k}$ from DPSelect is added to the attention weights before selecting the key-value pairs to retain:

$$\bar{\mathbf{a}} = \bar{\mathbf{a}} + \mathbf{M} \cdot \infty. \quad (8)$$

Further, we select the indices of the top- l' attention weights to retain as the new KVcache.

$$\mathbf{I} = \text{top-k}(\bar{\mathbf{a}}, l', \text{dim} = -1) \quad (9)$$

Based on the selected indices, we can extract the corresponding key and value states from the cache:

$$\begin{aligned} \mathbf{K}' &= \text{gather}(\mathbf{K}_{\text{cache},:, -l_q:, :}, \mathbf{I}) \\ \mathbf{V}' &= \text{gather}(\mathbf{V}_{\text{cache},:, -l_q:, :}, \mathbf{I}) \end{aligned} \quad (10)$$

The final step updates the KV cache by retaining the uncompressed part and appending the compressed part:

$$\begin{aligned} \mathbf{K}_{\text{cache},:, l_k - l_q:, :} &= \mathbf{K}' \\ \mathbf{V}_{\text{cache},:, l_v - l_q:, :} &= \mathbf{V}' \end{aligned} \quad (11)$$

Here, the prefill phase of the proposed RETAKE has been completed. The compressed KV cache obtained from previous steps enters the decoding phase, where the final answer is generated in an autoregressive manner.

4. Experiments

4.1. Benchmarks and Implementations

Video-MME. Video Multi-Modal Evaluation (Video-MME) [9] is a pioneering benchmark designed for evaluating MLLMs in video analysis, with diverse video types, and durations. It comprises 900 videos totaling 256 hours, with 2,700 manually labeled complex multiple-choice question-answer pairs across 30 subfields. It has three subsets of different durations: short (< 2min), medium (4min ~ 15min), and long (30min ~ 60min). **MLVU.** Multi-task Long Video Understanding Benchmark (MLVU) [52] has the widest range of video length ranging from 3 minutes to 2 hours. MLVU includes nine evaluation tasks including topic reasoning, anomaly recognition, video summarization, and plot question-answering. **LVBench.** LVBench [40] is a comprehensive benchmark for long video understanding, with an average video length of 4,101 seconds—4 times longer than VideoMME [9] and 5 times longer than MLVU [52]. It includes 1,549 annotated multiple-choice question-answer pairs covering a wide range of tasks, including entity recognition, event understanding, key information retrieval, temporal grounding, and reasoning.

Implementation details. Our experiments are based on QWen2-VL-7B [39] extended with RETAKE. Following the standard settings, we resized the longer side of the input frames to 448 pixels. We densely sampled the video at 2 frames per second (fps), with a maximum of 1024 frames. For our main results (Sec. 4.2), we used a 2x compression rate for RETAKE. In the ablation studies (Sec. 4.3), we reduced the maximum number of sampled frames to 512, as the maximum number of frames that can be processed without any multimodal content compression is approximately 300. All experiments were conducted on a single A100 GPU. More details are available in our code repository.

4.2. Main Results

Comparison with SoTAs. Experiment results on VideoMME [9], MLVU [52], and LVBench [40] are presented in Table 1 and Table 2, respectively. It can be observed that RETAKE consistently outperforms the existing best similar-size videoLLMs (e.g., LongVA [49], LongVILA-7B [45], LLaVA-OneVision-7B [16], and MiniCPM-V-2.6-8B [46]) with large margins of 3.0% ~ 4.9% on all benchmarks, even among videos of different durations and question types. RETAKE even outperforms the videoLLMs with much larger size, such as InternVL2-34B [13] and VideoLLaNA2-72B [7] in VideoMME [9], LLaVA-Onevision-72B [16] in MLVU [52]. Furthermore, RETAKE achieves performance comparable to GPT-4o-mini on VideoMME, and significantly surpasses strong GPT-4o on both MLVU and LVBench.

Table 1. Performance comparison in VideoMME [9] benchmark. “Size” refers to the number of parameters in LLM only. “S”, “M”, and “L” refer to the subsets of short, medium, and long duration, respectively.

Models	Size	S	M	L	Avg
<i>Proprietary Models</i>					
GPT-4V [1]	-	70.5	55.8	53.5	59.9
GPT-4o mini [29]	-	72.5	63.1	58.6	64.8
GPT-4o [29]	-	80.0	70.3	65.3	71.9
Gemini 1.5 Pro [31]	-	81.7	74.3	67.4	75.0
<i>Open-source Models</i>					
VideoChat2-Mistral [19]	7B	48.3	37.0	33.2	39.5
ShareGPT4Video [4]	8B	48.3	36.3	35.0	39.9
Video-LLaVA [22]	7B	45.3	38.0	36.2	39.9
Chat-UniVi-v1.5 [14]	7B	45.7	40.3	35.8	40.6
Qwen-VL-Chat [2]	7B	46.9	38.7	37.8	41.1
ShareGemini [34]	7B	49.1	41.3	39.1	43.2
SliMECASIA [50]	8B	53.3	42.7	39.8	45.3
Qwen-VL-Max [3]	-	55.8	49.2	48.9	51.3
LongVA [49]	7B	61.1	50.4	46.2	52.6
Long-LLaVA [42]	7B	61.9	51.4	45.4	52.9
Kangaroo [25]	8B	66.1	55.3	46.6	56.0
LongVILA [45]	7B	69.3	56.1	47.0	57.5
LLaVA-OneVision [16]	7B	-	-	-	58.2
MiniCPM-V 2.6 [46]	8B	71.3	59.4	51.8	60.9
Qwen2-VL [39]	7B	72.2	60.8	52.1	61.7
InternVL2 [13]	34B	72.0	59.1	52.6	61.2
VideoLLaMA 2 [6]	72B	69.8	59.9	57.6	62.4
RETAKE	7B	72.8	62.7	56.2	63.9
LLaVA-OneVision [16]	72B	76.7	62.2	60.0	66.3
Qwen2-VL [39]	72B	80.1	71.3	62.2	71.2

In-depth analysis. We provide an in-depth analysis of RETAKE on its performance across varying video lengths and question types. From Table 1, we find that the performance improvements of our method grow with video length. Specifically, RETAKE relatively outperforms MiniCPM-V [46] by 2.1% in the short subset, and by 5.6% and 8.5% in the medium and long subsets, respectively. Given that videos in the long subset range from 30 to 60 minutes, we believe these gains stem from our method’s ability to effectively process larger numbers of input frames as video length increases.

From Table 2, we observe that our method excels in tasks requiring detailed video understanding. For instance, in multi-detail questions from MLVU [52], RETAKE outperforms the closest method, TimeMarker [38], by 5.8% in action order (AO) and 5.3% in action count (AC). Moreover, RETAKE is only 0.2% lower than Oryx-1.5-34B [26] in needle QA (NQA) and even 0.9% higher in plot QA (PQA). These results suggest that RETAKE effectively preserves low-level details through PDSelect, and reduces high-level redundancy using PivotKV.

Table 2. Performance comparison in MLVU [52] and LVBench [40] benchmark. “Size” refers to the number of parameters in LLM only. Task categories in MLVU contain [40] TR–Topic Reasoning, AR–Anomaly Recognition, NQA–Needle Question-Answering, ER–Ego Reasoning, PQA–Plot Question-Answering, AO–Action Order, and AC–Action Count. Task categories in LVBench [40] contain ER–Entity Recognition, EU–Event Understanding, KIR–Key Information Retrieval, TG–Temporal Grounding, and Rea–Reasoning.

Methods	Size	MLVU								LVBench						
		Holistic		Single Detail			Multi Detail			Avg	ER	EU	KIR	TG	Rea	Avg
		TR	AR	NQA	ER	PQA	AO	AC								
<i>Proprietary Models</i>																
Qwen-VL-Max [3]	-	67.4	63.5	40.3	40.9	43.3	25.0	14.8	42.2	-	-	-	-	-	-	
GPT-4 Turbo [1]	-	79.5	68.0	45.9	47.4	60.6	26.5	16.1	49.2	26.5	23.7	28.3	21.4	28.0	27.0	
GPT-4o [29]	-	87.4	74.5	64.8	57.1	65.1	56.7	46.3	64.6	33.0	27.4	34.5	25.0	27.5	30.8	
Gemini 1.5 Pro [31]	-	-	-	-	-	-	-	-	-	32.1	30.9	39.3	31.8	27.0	33.1	
<i>Open-source Models</i>																
Otter-V [15]	7B	24.6	26.0	28.2	27.6	22.3	15.1	26.7	24.4	-	-	-	-	-	-	
MovieChat [36]	7B	29.5	25.0	24.2	24.7	25.8	28.6	22.8	25.8	21.3	23.1	25.9	22.3	24.0	22.5	
Movie-LLM [37]	7B	30.0	29.0	29.6	24.7	24.1	20.5	24.8	26.1	-	-	-	-	-	-	
TimeChat [33]	7B	23.1	27.0	24.5	28.4	25.8	24.7	32.0	30.9	21.9	21.7	25.9	22.7	25.0	22.3	
LLaMA-VID [21]	7B	50.8	34.5	30.1	32.7	32.5	23.9	27.8	33.2	25.4	21.7	23.4	26.4	26.5	23.9	
Video-LLaMA-2 [6]	7B	54.5	41.5	39.4	33.5	35.4	18.5	25.7	35.5	-	-	-	-	-	-	
MA-LMM [11]	7B	51.9	35.5	43.1	38.9	35.8	25.1	24.3	36.4	-	-	-	-	-	-	
LLaVA-1.6 [24]	7B	60.6	41.0	43.1	38.4	41.0	25.5	25.7	39.3	30.1	31.2	34.1	31.4	35.0	32.2	
VideoChat2 [19]	7B	74.6	51.5	42.0	47.4	43.8	22.8	29.6	44.5	-	-	-	-	-	-	
Video-LLaVA [22]	7B	71.6	57.0	53.2	45.2	48.4	20.1	35.9	47.3	-	-	-	-	-	-	
InternVL-1.5 [5]	20B	78.8	67.0	52.7	43.5	54.4	32.8	23.8	50.4	37.4	39.7	43.4	31.4	42.5	39.6	
VILA-1.5 [45]	40B	72.8	59.6	70.6	53.2	64.7	42.5	33.4	56.7	-	-	-	-	-	-	
CogVLM2 [12]	8B	-	-	-	-	-	-	-	-	28.3	27.1	31.0	25.5	25.5	28.1	
LongVA [49]	7B	81.5	66.6	77.9	60.6	73.8	49.3	34.8	63.5	-	-	-	-	-	-	
TimeMarker [38]	8B	82.7	65.9	79.9	58.7	74.9	49.7	35.5	63.9	42.8	39.1	34.9	38.7	38.2	41.3	
Qwen2-VL [39]	7B	86.0	62.5	81.9	63.6	71.8	53.3	34.5	64.8	44.0	41.6	43.0	39.1	43.3	42.4	
Video-XL [35]	7B	83.5	68.2	81.8	66.2	75.5	48.5	30.6	64.9	-	-	-	-	-	-	
LLaVA-Onevision [16]	72B	84.7	70.6	82.0	63.1	75.3	48.7	40.4	66.4	-	-	-	-	-	-	
RETAKE	7B	86.0	69.0	83.9	67.0	78.1	52.6	37.4	68.3	47.1	44.8	49.1	41.8	47.3	46.2	
Aria [17]	25B	93.3	73.9	88.4	66.0	81.2	51.6	39.8	70.6	-	-	-	-	-	-	
Oryx-1.5 [26]	34B	89.2	73.5	84.1	71.7	77.4	57.7	52.5	72.3	27.4	29.2	32.1	29.1	34.0	30.4	

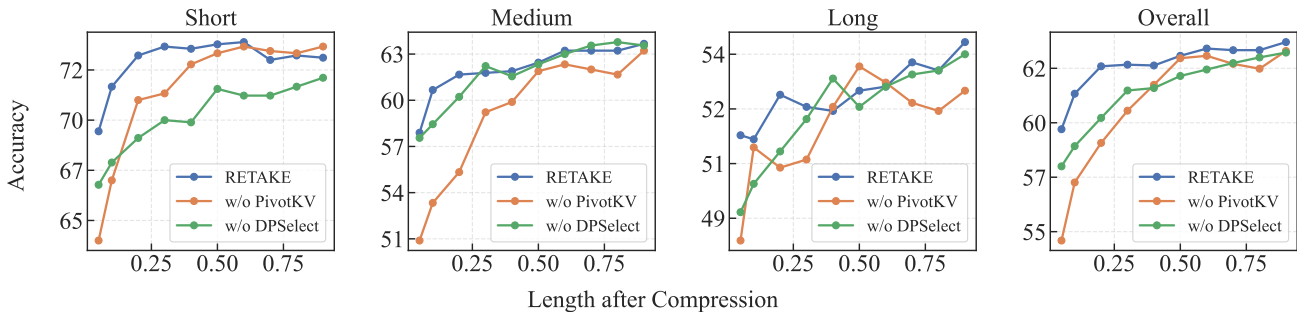


Figure 3. Performance of DPSelect and PivotKV under different compression ratios in different duration subsets of VideoMME [9].

4.3. Ablation Studies

Performance with different compression ratios. This section analyzes the impact of compression ratio on RETAKE across varying video lengths and task types, presented in Figure 3 and Figure 4, respectively. The experiments are conducted on the VideoMME dataset [9] with maximal sampled frames to be 512, which would have caused an OOM error without compression techniques.

The following findings can be observed: 1) On the overall performance, RETAKE enables a 4x compression ratio with less than 1% performance drop, which demonstrates the effectiveness of our method for multimodal content compression. 2) Even with an extremely high compression rate, i.e., reducing the video length to 0.05 of the original, the performance generally drops less than 3% among different video lengths and task types. This demonstrates the

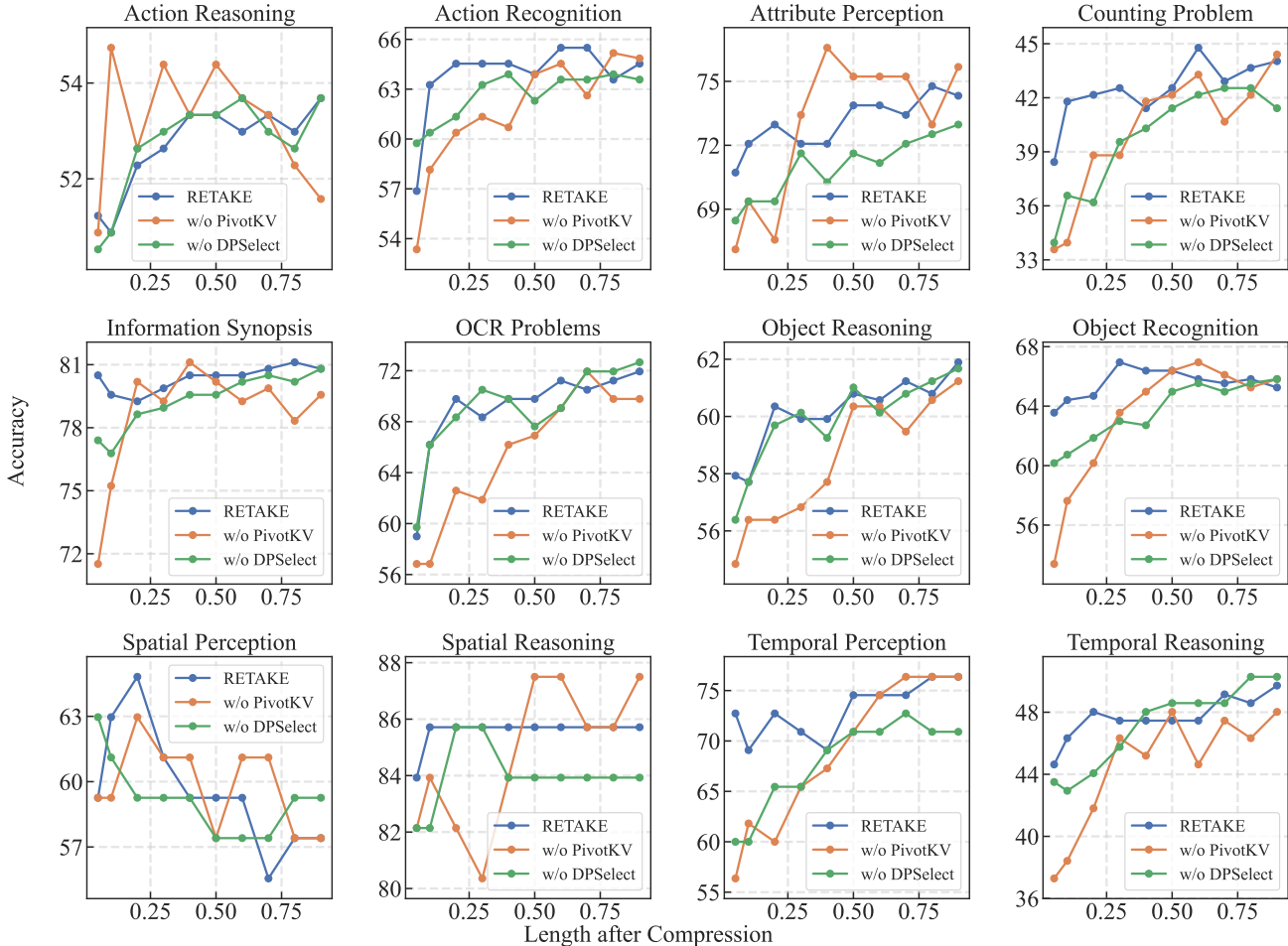


Figure 4. Performance of DPSelect and PivotKV under different compression ratios in different tasks in VideoMME [9] dataset.

robustness of RETAKE, benefiting from the jointly reducing temporal and knowledge redundancy. 3) For detail-oriented tasks like Action Recognition, Counting Problems, Object Recognition, and Short Videos, we notice an unusual phenomenon: compressing sequence length enhances performance compared to using the full model. This occurs because compression eliminates extraneous data, allowing the model to focus more precisely on crucial input elements, thereby improving feature identification and analysis.

Ablation of DPSelect and PivotKV. To investigate the roles of the components, we conduct experiments with two variants: "w/o DPSelect", where PivotKV omits DPSelect and summarizes KVCache using attention weights, and "w/o PivotKV", where only DPSelect is active.

The following observations can be made: 1) As shown in Table 1 and Table 2, RETAKE consistently outperforms our backbone Qwem2-VL with a significant margin across three datasets, especially on the longer video benchmarks

MLVU and LVBench. This validates the effectiveness of the combo of DPSelect and PivotKV. 2) On the overall performance in Figure 3, RETAKE performs better than both "w/o PivotKV" and "w/o DPSelect", especially at higher compression rates (lower length after compression). 3) The performance of "w/o PivotKV" drops significantly faster than "w/o DPSelect" and RETAKE. This demonstrates that simply reducing temporal redundancy contributes to much information loss. Thus, it is necessary to reduce knowledge redundancy for better performance under the same compression ratio. 4) As shown in Figure 3, RETAKE achieves similar results to "w/o DPSelect" in the medium and long subsets. However, in the short subset, RETAKE significantly outperforms "w/o DPSelect". This is because the short subset contains a higher proportion of perception questions, which demand more detailed low-level information to accurately interpret details or subtle changes. This shows that RETAKE excels in preserving low-level information, a benefit attributed to DPSelect.

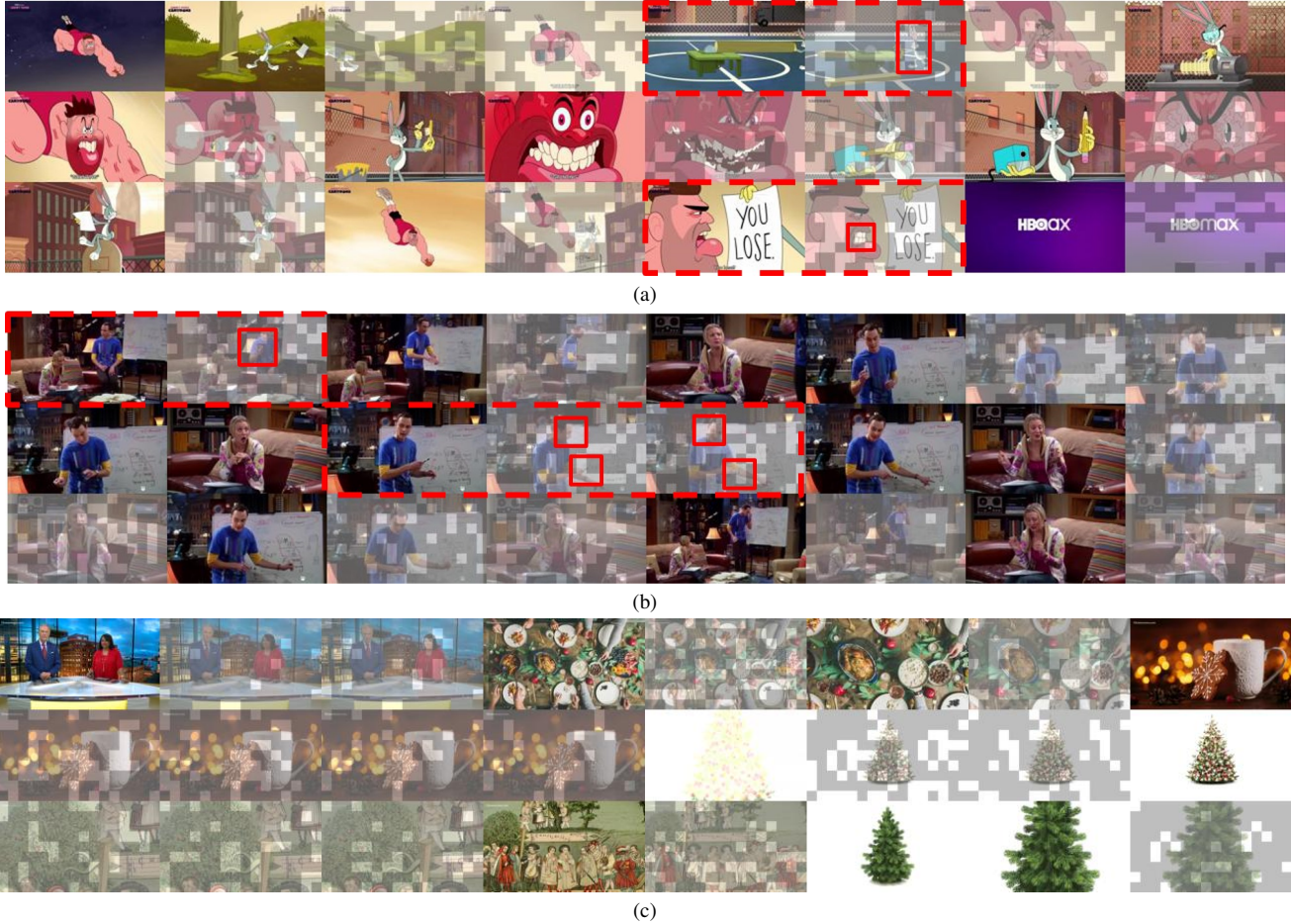


Figure 5. Visualization of how RETAKE reduce redundancies in video.

4.4. Visualization

To qualitatively evaluate the effectiveness of RETAKE, We present some visualization cases in Figure 5. The keyframes selected by DPSelect remain unchanged, while non-keyframes are painted white, and patches filtered by PivotKV are painted dark. From all cases in Figure 5, we can find that DPSelect can always effectively select important frames that differ from adjacent frames, filtering out redundant frames in static scenes. Besides, red boxes shows that PivotKV can always filters the patches similar to the keyframes and remains the patches with subtle semantic changes between non-keyframes and keyframes, such as body movement and facial expressions. For example, the region where a small animal appears (refer to the first red box of Figure 5a), and the area where the man’s mouth changes (refer to the second red box of Figure 5a), are identified and left uncompressed, while in red boxes of Figure 5b, the frequently changing facial and arm regions of the character are selected and preserved. This validates our initial motivation that DPSelect reduces low-level temporal redundancy and

PivotKV reduces high-level knowledge redundancy. However, there are no significant motions in Figure 5c, and as a result, the filtered token distribution is relatively sparse.

5. Conclusion

This paper introduces RETAKE, a training-free approach to understanding long videos by jointly reducing temporal and knowledge redundancy with two novel modules: DPSelect and PivotKV. DPSelect, inspired by human perception, identifies keyframes with significant motion peaks, while PivotKV compresses the KV cache of non-keyframes using knowledge-relevant attention scores. Experiments demonstrate that RETAKE can handle video sequences up to four times longer with less than 1% performance loss, outperforming 7B-scale videoLLMs like recent MiniCPM-V2.6-8B and LLaVA-OneVision-7B, while also competing with larger videoLLMs like InternVL2-34B and VideoLLaMA 2-72B and GPT-4o. RETAKE presents a novel approach to long video understanding, offering improved efficiency and achieving state-of-the-art performance.

References

- [1] Josh Achiam, Steven Adler, Sandhini Agarwal, Lama Ahmad, Ilge Akkaya, Florencia Leoni Aleman, Diogo Almeida, Janko Altenschmidt, Sam Altman, Shyamal Anadkat, et al. Gpt-4 technical report, 2023. arXiv:2303.08774. 5, 6
- [2] Jinze Bai, Shuai Bai, Shusheng Yang, Shijie Wang, Sinan Tan, Peng Wang, Junyang Lin, Chang Zhou, and Jingren Zhou. Qwen-vl: A frontier large vision-language model with versatile abilities. *CoRR*, abs/2308.12966, 2023. 5
- [3] Jinze Bai, Shuai Bai, Yunfei Chu, Zeyu Cui, Kai Dang, Xiaodong Deng, Yang Fan, Wenbin Ge, Yu Han, Fei Huang, et al. Qwen technical report, 2023. arXiv:2309.16609. 5, 6
- [4] Lin Chen, Xilin Wei, Jinsong Li, Xiaoyi Dong, Pan Zhang, Yuhang Zang, Zehui Chen, Haodong Duan, Bin Lin, Zhenyu Tang, Li Yuan, Yu Qiao, Dahua Lin, Feng Zhao, and Jiaqi Wang. Sharegpt4video: Improving video understanding and generation with better captions. *CoRR*, abs/2406.04325, 2024. 5
- [5] Zhe Chen, Weiyun Wang, Hao Tian, Shenglong Ye, Zhangwei Gao, Erfei Cui, Wenwen Tong, Kongzhi Hu, Jiapeng Luo, Zheng Ma, Ji Ma, Jiaqi Wang, Xiaoyi Dong, Hang Yan, Hwei Guo, Conghui He, Botian Shi, Zhenjiang Jin, Chao Xu, Bin Wang, Xingjian Wei, Wei Li, Wenjian Zhang, Bo Zhang, Pinlong Cai, Licheng Wen, Xiangchao Yan, Min Dou, Lewei Lu, Xizhou Zhu, Tong Lu, Dahua Lin, Yu Qiao, Jifeng Dai, and Wenhai Wang. How far are we to gpt-4v? closing the gap to commercial multimodal models with open-source suites. *CoRR*, abs/2404.16821, 2024. 6
- [6] Zesen Cheng, Sicong Leng, Hang Zhang, Yifei Xin, Xin Li, Guanzheng Chen, Yongxin Zhu, Wenqi Zhang, Ziyang Luo, Deli Zhao, and Lidong Bing. Videollama 2: Advancing spatial-temporal modeling and audio understanding in video-llms. *CoRR*, abs/2406.07476, 2024. 5, 6
- [7] Zesen Cheng, Sicong Leng, Hang Zhang, et al. Videollama 2: Advancing spatial-temporal modeling and audio understanding in video-llms, 2024. arXiv:2406.07476. 2, 5
- [8] Wei-Lin Chiang, Zhuohan Li, Zi Lin, Ying Sheng, Zhanghao Wu, Hao Zhang, Lianmin Zheng, Siyuan Zhuang, Yonghao Zhuang, Joseph E Gonzalez, et al. Vicuna: An open-source chatbot impressing gpt-4 with 90%* chatgpt quality. See <https://vicuna.lmsys.org> (accessed 14 April 2023), 2(3):6, 2023. 2
- [9] Chaoyou Fu, Yuhan Dai, Yondong Luo, Lei Li, Shuhuai Ren, Renrui Zhang, Zihan Wang, Chenyu Zhou, Yunhang Shen, Mengdan Zhang, Peixian Chen, Yanwei Li, Shaohui Lin, Sirui Zhao, Ke Li, Tong Xu, Xiawu Zheng, Enhong Chen, Rongrong Ji, and Xing Sun. Video-mme: The first-ever comprehensive evaluation benchmark of multi-modal llms in video analysis. *CoRR*, abs/2405.21075, 2024. 2, 5, 6, 7
- [10] Rafael C Gonzales and Paul Wintz. *Digital image processing*. Addison-Wesley Longman Publishing Co., Inc., 1987. 2
- [11] Bo He, Hengduo Li, Young Kyun Jang, Menglin Jia, Xuefei Cao, Ashish Shah, Abhinav Shrivastava, and Ser-Nam Lim. MA-LMM: Memory-Augmented Large Multimodal Model for Long-Term Video Understanding. In *Computer Vision and Pattern Recognition*, pages 13504–13514. IEEE, 2024. 1, 2, 3, 6
- [12] Wenyi Hong, Weihang Wang, Ming Ding, Wenmeng Yu, Qingsong Lv, Yan Wang, Yean Cheng, Shiyu Huang, Junhui Ji, Zhao Xue, et al. Cogvlm2: Visual language models for image and video understanding, 2024. arXiv:2408.16500. 6
- [13] Internvl2. Internvl2: Better than the best—expanding performance boundaries of open-source multimodal models with the progressive scaling strategy, 2024. Accessed: 2024-11-13. 2, 5
- [14] Peng Jin, Ryuichi Takanobu, Wancai Zhang, Xiaochun Cao, and Li Yuan. Chat-univi: Unified visual representation empowers large language models with image and video understanding. In *CVPR*, pages 13700–13710. IEEE, 2024. 1, 3, 5
- [15] Bo Li, Yuanhan Zhang, Liangyu Chen, Jinghao Wang, Jingkang Yang, and Ziwei Liu. Otter: A multi-modal model with in-context instruction tuning. *CoRR*, abs/2305.03726, 2023. 6
- [16] Bo Li, Yuanhan Zhang, Dong Guo, Renrui Zhang, Feng Li, Hao Zhang, Kaichen Zhang, Yanwei Li, Ziwei Liu, and Chunyuan Li. LLaVA-OneVision: Easy Visual Task Transfer, 2024. arXiv:2408.03326. 1, 2, 5, 6
- [17] Dongxu Li, Yudong Liu, Haoning Wu, Yue Wang, Zhiqi Shen, Bowen Qu, Xinyao Niu, Guoyin Wang, Bei Chen, and Junnan Li. Aria: An open multimodal native mixture-of-experts model, 2024. arXiv:2410.05993. 6
- [18] KunChang Li, Yanan He, Yi Wang, Yizhuo Li, Wenhai Wang, Ping Luo, Yali Wang, Limin Wang, and Yu Qiao. Videochat: Chat-centric video understanding, 2024. arXiv:2305.06355. 1, 2
- [19] Kunchang Li, Yali Wang, Yanan He, Yizhuo Li, Yi Wang, Yi Liu, Zun Wang, Jilan Xu, Guo Chen, Ping Lou, Limin Wang, and Yu Qiao. Mvbench: A comprehensive multimodal video understanding benchmark. In *CVPR*, pages 22195–22206. IEEE, 2024. 1, 2, 5, 6
- [20] Yuhong Li, Yingbing Huang, Bowen Yang, Bharat Venkitesh, Acyr Locatelli, Hanchen Ye, Tianle Cai, Patrick Lewis, and Deming Chen. SnapKV: LLM Knows What You are Looking for Before Generation, 2024. arXiv:2404.14469. 2
- [21] Yanwei Li, Chengyao Wang, and Jiaya Jia. Llama-vid: An image is worth 2 tokens in large language models. In *ECCV (46)*, pages 323–340. Springer, 2024. 2, 6
- [22] Bin Lin, Yang Ye, Bin Zhu and Jiayi Cui, Munan Ning, Peng Jin, and Li Yuan. Video-llava: Learning united visual representation by alignment before projection, 2023. arXiv:2311.10122. 1, 2, 5, 6
- [23] Haotian Liu, Chunyuan Li, Qingyang Wu, and Yong Jae Lee. Visual instruction tuning, 2023. arXiv:2304.08485. 1
- [24] Haotian Liu, Chunyuan Li, Yuheng Li, Bo Li, Yuanhan Zhang, Sheng Shen, and Yong Jae Lee. Llava-next: Improved reasoning, ocr, and world knowledge, 2024. 2, 6
- [25] Jiajun Liu, Yibing Wang, Hanghang Ma, Xiaoping Wu, Xiaohu Ma, Xiaoming Wei, Jianbin Jiao, Enhua Wu, and Jie Hu. Kangaroo: A powerful video-language model supporting long-context video input. *CoRR*, abs/2408.15542, 2024. 5

- [26] Zuyan Liu, Yuhao Dong, Ziwei Liu, Winston Hu, Jiwen Lu, and Yongming Rao. Oryx mllm: On-demand spatial-temporal understanding at arbitrary resolution, 2024. arXiv:2409.12961. 5, 6
- [27] Zhong-Lin Lu and George Sperling. The functional architecture of human visual motion perception. *Vision research*, 35: 2697–2722, 1995. 2
- [28] Muhammad Maaz, Hanoona Abdul Rasheed, Salman Khan, and Fahad Khan. Video-chatgpt: Towards detailed video understanding via large vision and language models. In *ACL (1)*, pages 12585–12602. Association for Computational Linguistics, 2024. 1, 2
- [29] OpenAI. Gpt-4o. <https://openai.com/index/hello-gpt-4o/>, 2024. 5, 6
- [30] Alec Radford, Jong Wook Kim, Chris Hallacy, Aditya Ramesh, Gabriel Goh, Sandhini Agarwal, Girish Sastry, Amanda Askell, Pamela Mishkin, Jack Clark, Gretchen Krueger, and Ilya Sutskever. Learning transferable visual models from natural language supervision. In *ICML*, pages 8748–8763. PMLR, 2021. 2
- [31] Machel Reid, Nikolay Savinov, Denis Teplyashin, Dmitry Lepikhin, Timothy P. Lillicrap, Jean-Baptiste Alayrac, Radu Soricut, Angeliki Lazaridou, Orhan Firat, Julian Schrittwieser, Ioannis Antonoglou, Rohan Anil, Sebastian Borgeaud, Andrew M. Dai, Katie Millican, Ethan Dyer, Mia Glaese, Thibault Sottiaux, Benjamin Lee, Fabio Viola, Malcolm Reynolds, Yuanzhong Xu, James Molloy, Jilin Chen, Michael Isard, Paul Barham, Tom Hennigan, Ross McIlroy, Melvin Johnson, Johan Schalkwyk, Eli Collins, Eliza Rutherford, Erica Moreira, Kareem Ayoub, Megha Goel, Clemens Meyer, Gregory Thornton, Zhen Yang, Henryk Michalewski, Zaheer Abbas, Nathan Schucher, Ankesh Anand, Richard Ives, James Keeling, Karel Lenc, Salem Haykal, Siamak Shakeri, Pranav Shyam, Aakanksha Chowdhery, Roman Ring, Stephen Spencer, Eren Sezener, and et al. Gemini 1.5: Unlocking multimodal understanding across millions of tokens of context. *CoRR*, abs/2403.05530, 2024. 5, 6
- [32] Shuhuai Ren, Sishuo Chen, Shicheng Li, Xu Sun, and Lu Hou. TESTA: temporal-spatial token aggregation for long-form video-language understanding. In *EMNLP (Findings)*, pages 932–947. Association for Computational Linguistics, 2023. 3
- [33] Shuhuai Ren, Linli Yao, Shicheng Li, Xu Sun, and Lu Hou. Timechat: A time-sensitive multimodal large language model for long video understanding, 2023. arXiv:2312.02051. 6
- [34] Share14. Sharegemini: Scaling up video caption data for multimodal large language models, 2024. Accessed: 2024-11-11. 5
- [35] Yan Shu, Peitian Zhang, Zheng Liu, Minghao Qin, Junjie Zhou, Tiejun Huang, and Bo Zhao. Video-XL: Extra-Long Vision Language Model for Hour-Scale Video Understanding, 2024. arXiv:2409.14485. 1, 2, 6
- [36] Enxin Song, Wenhao Chai, Guanhong Wang, Yucheng Zhang, Haoyang Zhou, Feiyang Wu, Haozhe Chi, Xun Guo, Tian Ye, Yanting Zhang, Yan Lu, Jenq-Neng Hwang, and Gaoang Wang. Moviechat: From dense token to sparse memory for long video understanding. In *CVPR*, pages 18221–18232. IEEE, 2024. 1, 3, 6
- [37] Zhende Song, Chenchen Wang, Jiamu Sheng, Chi Zhang, Gang Yu, Jiayuan Fan, and Tao Chen. MovieLLM: Enhancing long video understanding with ai-generated movies, 2024. arXiv:2403.01422. 6
- [38] TimeMarker-LLM. Timemarker: A versatile video-llm for long and short video understanding with superior temporal localization ability, 2024. Accessed: 2024-11-13. 5, 6
- [39] Peng Wang, Shuai Bai, Sinan Tan, Shijie Wang, Zhihao Fan, Jinze Bai, Keqin Chen, Xuejing Liu, Jialin Wang, Wenbin Ge, Yang Fan, Kai Dang, Mengfei Du, Xuancheng Ren, Rui Men, Dayiheng Liu, Chang Zhou, Jingren Zhou, and Junyang Lin. Qwen2-VL: Enhancing Vision-Language Model’s Perception of the World at Any Resolution, 2024. arXiv:2409.12191. 1, 5, 6
- [40] Weihang Wang, Zehai He, Wenyi Hong, Yean Cheng, Xiaohan Zhang, Ji Qi, Shiyu Huang, Bin Xu, Yuxiao Dong, Ming Ding, and Jie Tang. Lvbench: An extreme long video understanding benchmark, 2024. 5, 6
- [41] Xiao Wang, Yaoyu Li, Tian Gan, Zheng Zhang, Jingjing Lv, and Liqiang Nie. RTQ: rethinking video-language understanding based on image-text model. In *International Conference on Multimedia*, pages 557–566. ACM, 2023. 1
- [42] Xidong Wang, Dingjie Song, Shunian Chen, Chen Zhang, and Benyou Wang. Longllava: Scaling multi-modal llms to 1000 images efficiently via hybrid architecture. *CoRR*, abs/2409.02889, 2024. 5
- [43] Yuetian Weng, Mingfei Han, Haoyu He, Xiaojun Chang, and Bohan Zhuang. LongVLM: Efficient Long Video Understanding via Large Language Models. In *European Conference of Computer Vision*, pages 453–470. Springer, 2024. 1, 2
- [44] Haoning Wu, Dongxu Li, Bei Chen, and Junnan Li. Longvideobench: A benchmark for long-context interleaved video-language understanding. *CoRR*, abs/2407.15754, 2024. 2
- [45] Fuzhao Xue, Yukang Chen, Dacheng Li, Qinghao Hu, Ligeng Zhu, Xiuyu Li, Yunhao Fang, Haotian Tang, Shang Yang, Zhijian Liu, Ethan He, Hongxu Yin, Pavlo Molchanov, Jan Kautz, Linxi Fan, Yuke Zhu, Yao Lu, and Song Han. Longvila: Scaling long-context visual language models for long videos, 2024. arXiv:2408.10188. 1, 2, 5, 6
- [46] Yuan Yao, Tianyu Yu, Ao Zhang, Chongyi Wang, Junbo Cui, Hongji Zhu, Tianchi Cai, Haoyu Li, Weilin Zhao, Zhihui He, Qianyu Chen, Huarong Zhou, Zhensheng Zou, Haoye Zhang, Shengding Hu, Zhi Zheng, Jie Zhou, Jie Cai, Xu Han, Guoyang Zeng, Dahai Li, Zhiyuan Liu, and Maosong Sun. Minicpm-v: A GPT-4V level MLLM on your phone. *CoRR*, abs/2408.01800, 2024. 2, 5
- [47] Zhiyuan Zeng, Qipeng Guo, Xiaoran Liu, Zhangyue Yin, Wentao Shu, Mianqiu Huang, Bo Wang, Yunhua Zhou, Lintin Li, Qun Liu, et al. Memorize step by step: Efficient long-context prefilling with incremental memory and decremental chunk. In *Proceedings of the Conference on Empirical Methods in Natural Language Processing*, pages 21021–21034. ACL, 2024. 3

- [48] Hang Zhang, Xin Li, and Lidong Bing. Video-llama: An instruction-tuned audio-visual language model for video understanding. In *EMNLP (Demos)*, pages 543–553. Association for Computational Linguistics, 2023. [1](#)
- [49] Peiyuan Zhang, Kaichen Zhang, Bo Li, Guangtao Zeng, Jingkang Yang, Yuanhan Zhang, Ziyue Wang, Haoran Tan, Chunyuan Li, and Ziwei Liu. Long Context Transfer from Language to Vision, 2024. [arXiv:2406.16852](#). [1](#), [2](#), [5](#), [6](#)
- [50] Yi-Fan Zhang, Qingsong Wen, Chaoyou Fu, Xue Wang, Zhang Zhang, Liang Wang, and Rong Jin. Beyond llava-hd: Diving into high-resolution large multimodal models. *CoRR*, [abs/2406.08487](#), 2024. [5](#)
- [51] Zhenyu Zhang, Ying Sheng, Tianyi Zhou, Tianlong Chen, Lianmin Zheng, Ruisi Cai, Zhao Song, Yuandong Tian, Christopher Ré, Clark W. Barrett, Zhangyang Wang, and Beidi Chen. H2O: Heavy-Hitter Oracle for Efficient Generative Inference of Large Language Models. In *Advances in Neural Information Processing Systems*, 2023. [2](#)
- [52] Junjie Zhou, Yan Shu, Bo Zhao, Boya Wu, Shitao Xiao, Xi Yang, Yongping Xiong, Bo Zhang, Tiejun Huang, and Zheng Liu. MLVU: A comprehensive benchmark for multi-task long video understanding. *CoRR*, [abs/2406.04264](#), 2024. [2](#), [5](#), [6](#)
- [53] Heqing Zou, Tianze Luo, Guiyang Xie, Victor, Zhang, Fengmao Lv, Guangcong Wang, Juanyang Chen, Zhuochen Wang, Hansheng Zhang, and Huaijian Zhang. From Seconds to Hours: Reviewing MultiModal Large Language Models on Comprehensive Long Video Understanding, 2024. [arXiv:2409.18938](#). [1](#)